Proton beam characterization in the experimental room of the Trento Proton Therapy facility

F. Tommasino [a,b,*], M. Rovituso [b], S. Fabiano [b,c], S. Piffer [a,b], C. Manea [b], S. Lorentini [d], S. Lanzone [e], Z. Wang [e], M. Pasini [e], W.J. Burger [b,f], C. La Tessa [a,b], E. Scifoni [b], M. Schwarz [b,d], M. Durante [b]

[a] Department of Physics, University of Trento, Povo, Italy
[b] Trento Institute for Fundamental Physics and Applications (TIFPA), National Institute for Nuclear Physics, (INFN), Povo, Italy
[c] Department of Physics and Astronomy, University of Catania, Catania, Italy
[d] Protontherapy Department, Azienda Provinciale per i Servizi Sanitari (APSS), Trento, Italy
[e] Ion Beam Applications (IBA), Louvain-la-Neuve, Belgium
[f] Bruno Kessler Foundation (FBK), Trento, Italy

A B S T R A C T

As proton therapy is becoming an established treatment methodology for cancer patients, the number of proton centres is gradually growing worldwide. The economical effort for building these facilities is motivated by the clinical aspects, but might be also supported by the potential relevance for the research community. Experiments with high-energy protons are needed not only for medical physics applications, but represent also an essential part of activities dedicated to detector development, space research, radiation hardness tests, as well as of fundamental research in nuclear and particle physics.

Here we present the characterization of the beam line installed in the experimental room of the Trento Proton Therapy Centre (Italy). Measurements of beam spot size and envelope, range verification and proton flux were performed in the energy range between 70 and 228 MeV. Methods for reducing the proton flux from typical treatments values of 10^6–10^9 particles/s down to 10^1–10^5 particles/s were also investigated. These data confirm that a proton beam produced in a clinical centre build by a commercial company can be exploited for a broad spectrum of experimental activities. The results presented here will be used as a reference for future experiments.

1. Introduction

The Trento Proton Therapy facility, which is part of the Trentino Healthcare Agency (Azienda Provinciale per i Servizi Sanitari — APSS, Italy), started clinical operations in October 2014. A cyclotron (IBA, Proteus 235) serves two medical treatment rooms both equipped with rotating gantries, where more than 300 patients have been treated (number updated at March 2017) including paediatric patients [1].

The facility is also equipped with an experimental area where the beam line is split in two branches, both dedicated to a large spectrum of scientific applications, including medical physics, detector testing, radiation hardness measurements, space research and radiobiology. Following an institutional agreement with APSS, the beam is available in the experimental room outside clinical hours and all activities are managed and supervised by the Trento Institute for Fundamental Physics and Applications (TIFPA), which is part of the Italian National Institute for Nuclear Physics (INFN). Access to the research beam line is open to external users, in the framework of scientific collaborations or industrial applications, provided acceptance by the Program Advisory Committee (PAC) organized by TIFPA (http://www.tifpa.infn.it/sc-init/med-tech/p-beam-research/).

In parallel with the development and spread of charged particle therapy, several experimental irradiation rooms with ion beams at therapeutic energies have been setup worldwide in the last decades. The configuration where a pure clinical centre is hosting a research-dedicated beam line is very attractive for several reasons. First, it allows a close connection between experts dedicated to standardize clinical protocols and those involved in cutting-edge research for advancing proton therapy. Moreover, extending the use of ion beams to other

* Correspondence to: Department of Physics, University of Trento, via Sommarive 14, 38123 Povo, Italy.
E-mail address: francesco.tommasino@unitn.it (F. Tommasino).

types of research lower the cost burden of the facility itself. In Europe, experimental rooms are available at the Heavy Ion Therapy centre (HIT) of Heidelberg (Germany) [2], the University Proton Therapy Dresden (UPTD, Germany) [3], the Krakow Proton Therapy facility (IFJ PAN, Krakow, Poland) [4] and the CATANA line at the INFN-LNS (Laboratori Nazionali del Sud, Catania, Italy) [5]. While the first two are part of clinical centres, those located in Krakow and Catania were developed in the context of nuclear physics facilities, and started treating patients with ocular cancers [4,6]. All centres offer a proton beam, while heavier ions are available only at HIT and CATANA. Experimental rooms in other irradiation facilities are currently under commissioning, as in the National Centre for Oncological Hadrontherapy (CNAO, Pavia, Italy) [7]. At the same time, also USA [8] and Japan [9] are heavily investing in these types of combined centres.

The current solutions offered by commercial companies for proton centres setups are attracting a growing interest worldwide. This work shows how these types of facilities can be used beyond their clinical aim, paving the way for a new concept of combined radiotherapy and multidisciplinary research-oriented centre.

In this manuscript, the infrastructure of the experimental area will be shortly described. The procedure and results of the beam characterization of the Trento Proton Therapy centre will be also presented. This includes measurements of beam spot profiles in air, envelope, range verification and flux. These data represent a reference database that can be used by the scientific community for planning experimental activities as well as for future upgrades of the facility.

2. Materials and methods

2.1. Beam production and transport

Proton beam production and transport in the Trento facility are under the responsibility of the IBA company (Ion Beam Applications, Louvain-La-Neuve, Belgium), which produced and installed the related infrastructure. IBA is also responsible for beam operations and has a resident staff in the facility. The cyclotron accelerates the beam up to a maximum energy of 228 MeV. Shortly after the cyclotron exit, a coarse energy selection is carried-out by a rotating degrader of different thicknesses and materials in order to reduce the beam energy down to its minimum value of 70 MeV. This is part of an Energy Selection System (ESS) that allows the fine selection of the desired energy to be transported downstream. Two branches of the main line transport the beam to the gantries, while a third branch connects it to the experimental room. The beam cannot be shared simultaneously among the different rooms and can only be requested alternately in either the gantries or the research area. Different beam intensities can be requested at the exit of the cyclotron, in a range spanning between 1 and 320 nA. The proton beam current will be modulated by a 50% duty-cycle square wave, with a 100 ms period. These current values correspond to the charge collected by an ionization chamber that can be inserted in the beam line shortly after the cyclotron exit and before the ESS. Depending on the requested energy, a significant part of the beam could be lost during the selection process. Therefore, the intensity values reported above provide an indication of the dynamic range available but, because of the variable transport efficiency, do not always correspond to the number of protons delivered in the rooms. While calibrated monitor Ionization Chambers (IC) are installed in the gantries, dedicated measurements have been performed in the experimental room for evaluating proton flux in air at different energies.

A dedicated effort was done to investigate a methodology for delivering low beam intensities (i.e. fluxes in the order of $10^1 - 10^5$ particles/s) that are needed for a broad spectrum of experiments. This requires the accelerator to work in an operational regime that is different from the standard (clinical) one. In fact, such low intensities are obtained by exploiting the so-called accelerator "dark current", achieved by decreasing the high voltage of the accelerator source below the threshold used for standard operations. In this condition, a significantly smaller fraction of protons is extracted from the cyclotron and the monitoring devices along the beam line are not able to detect the particles. In this regime, a dedicated measurement system is needed for quantifying the proton flux (see Detectors Section below for details) within a range of 10^1–10^5 particles per second. When operating in this condition, the proton beam flux can be adjusted by fine-tuning the accelerator radio frequency voltage. This process can be done online by the operators, and usually only few minutes are required to find the optimal settings for the desired rate.

2.2. The experimental area

The experimental area consists of two different spaces: a multifunctional preparation room and the irradiation cave. The former is equipped with a control station for monitoring the activities inside the cave via remote control cameras and alignment lasers. Additionally, a patch panel equipped with 32 BNC, 12 SHV (max voltage 5 kV), 8 D-SUB and 8 Ethernet (1 Gb) cables connects the preparation room with the irradiation cave allowing the electronics installation for the data acquisition inside or outside the cave, according to the specific needs of the experiment. In case additional cables are needed, the path between the preparation room and the irradiation cave measures about 25 m.

The main beam line is split into two additional sub-branches at 0° and 30° with respect to its initial direction by a dipole magnet (Fig. 1(A)). This allows the simultaneous setup of two different experiments if necessary but the beam cannot be transported along the two branches at the same time. We refer to the 0° and to the 30° lines as the "Biology" and "Physics" beam line, respectively (Fig. 1(B)), since they are intended for different purposes and thus will be implemented with different hardware. In particular, the Biology line will require a broad homogeneous beam, able to homogeneously irradiate biological samples, while the Physics will mostly use a narrow spot. Results of Physics beam line characterization are presented in this work.

A fixed pencil beam is available at the Physics line with energies between 70 and 228 MeV selectable with the ESS. Further energy reduction is possible inside the cave using dedicated in-air degraders. Protons exit the beam pipe by traversing a 70 μm thickness titanium layer. Lasers are available for target alignment at 1.25 m from the exit window, which we define as "Isocenter" in analogy to the treatment rooms. Tables with adjustable heights are used for target positioning.

2.3. Detectors

A short description of the detectors used in this study and the corresponding measurements for which they were employed is reported below. Dedicated references are provided for additional information on the specific detector.

- Lynx (IBA-Dosimetry): scintillating screen coupled with charge-coupled device (CCD) cameras, sensitive area 30 cm × 30 cm, resolution of 0.5 mm in both X–Y plane, used for in air spot profile measurements [10].
- Giraffe (IBA-Dosimetry): multilayer IC, consisting of a stack of 180 independent parallel-plate IC with a 2 mm gap from each other (the gap also defines the raw data resolution), sensitive area of 10 cm diameter, used for range measurements [11].
- Mini-Q (DE.TEC.TOR): stack of coupled strips and integral IC for measuring profiles on the plane perpendicular to the beam direction, sensitive area of 14.7 cm × 14.7 cm; it was also used to quantify the proton flux after an appropriate calibration [12].
- Faraday Cup: in-house built basic configuration consisting of a shielded and insulated 6.35 cm thick Brass block, coupled with an electrometer for charge measurements (so-called "poor man Faraday Cup" [13]), adopted for cross calibration of the Mini-Q detector.

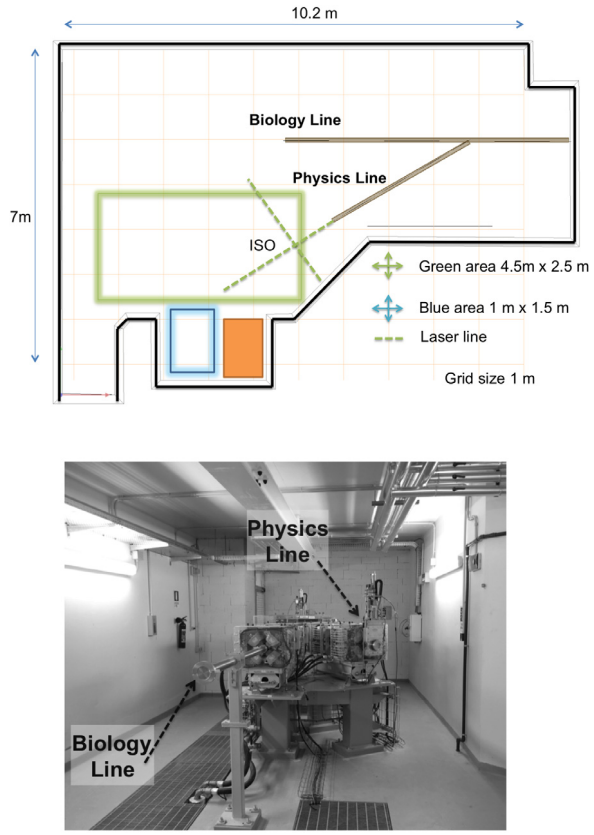

Fig. 1. A picture (upper panel) and a schematic view (lower panel) of the experimental room at the Trento Protontherapy centre. The Biology (0° branch) and Physics (30° branch) beam lines are indicated. In the map the space available for experimental setup at the Physics line is indicated (green area), together with an additional area for equipment storage inside the cave during irradiation (blue area). (For interpretation of the references to colour in this figure legend, the reader is referred to the web version of this article.)

The Lynx, Giraffe and Mini-Q detectors are equipped with read-out electronics as well as with dedicated software for the data acquisition. Additionally, a plastic scintillator (EJ200, Eljen, USA) coupled with a photomultiplier tube (H7415, Hamamatsu, Japan) was employed to characterize the beam rate at low intensities. The data were recorded event-by-event using a NIM-based acquisition system and analysed with the ROOT software. The scintillator analog signal was split into two branches in order to acquire the energy spectrum and the beam rate. The pulse height of each signal was recorded with an Analog to Digital Converter (ADC, Ortec 927 Aspec MCA, USA) after being amplified (Tennelec TC 248, USA) and centred in a proper gate produced by a Gate Generator (Ortec 8020, USA). The discriminated signal (Leading Edge discriminator Philips 730) of the scintillator was acquired with a scaler (Ortec 871, USA) to assess the number of incident protons.

3. Results

3.1. Range verification

Pseudo-monoenergetic pencil beams in the energy range 70–228 MeV were measured with the Giraffe detector. By means of a previous calibration against range measurements in a water phantom with a Bragg peak chamber, the Giraffe software returns the proton range in water (expressed as R90, corresponding to the position in the distal fall-off of the Bragg curve where the dose is reduced to 90% of the peak maximum). The pencil beam energy can be then reconstructed from this value. These measurements provided an evaluation of the shift between the nominal energy (i.e. the value just after the ESS,

Table 1
Nominal and effective values of the beam energy and corresponding range and maximum flux. The former refer to the energy at the cyclotron exit while the latter are measured in the experimental room at the Isocenter position. Flux measurements in the last column refer to 1 nA beam extraction current. The extraction current can be increased up to 320 nA, and the flux can scale consequently.

Nominal values		Effective valuesat ISO		Flux (p/s)
E (MeV)	R90 (g/cm^2)	E (MeV)	R90 (g/cm^2)	
70.2	4.1	68.5	3.9	3.8×10^6
73.9	4.5	72.4	4.3	–
82.7	5.5	82.3	5.4	7.5×10^6
90.8	6.5	89.5	6.3	9.9×10^6
100.0	7.5	98.6	7.5	1.2×10^7
105.6	8.5	104.2	8.3	–
112.4	9.5	11.2	9.3	2.1×10^7
119.0	10.5	117.8	10.3	2.8×10^7
125.3	11.5	124.1	11.3	–
131.3	12.5	130.3	12.3	2.7×10^7
137.2	13.5	136.1	13.3	–
142.9	14.5	141.7	14.2	3.6×10^7
148.5	15.5	147.1	15.2	–
153.9	16.5	152.7	16.2	4.6×10^7
159.2	17.5	158.0	17.2	5.5×10^7
164.4	18.5	163.1	18.2	–
169.4	19.5	168.1	19.2	7.4×10^7
174.4	20.5	173.4	20.2	–
179.3	21.5	178.2	21.2	9.0×10^7
184.1	22.5	182.8	22.2	–
188.8	23.5	187.4	23.2	1.1×10^8
193.4	24.5	192.3	24.2	–
197.9	25.5	196.8	25.2	–
202.4	26.5	201.1	26.1	1.4×10^8
206.9	27.5	205.6	27.1	–
211.2	28.5	210.0	28.1	1.7×10^8
215.5	29.5	214.2	29.1	–
219.8	30.5	218.4	30.1	2.0×10^8
224.0	31.5	222.9	31.2	–
228.2	32.5	227.4	32.3	2.3×10^8

the corresponding range was obtained by measuring Bragg peak curves in a water phantom positioned at the exit of the ESS during the construction of the facility) and the actual energy of the beam at the Isocenter. The discrepancy between the values is slightly dependent on the energy itself, as shown in Table 1. The Peak-to Plateau ratios were calculated for the Bragg curves shown in Fig. 2 and are summarized in Table 2. The gradual decrease in peak height at increasing beam energies comes from both inelastic nuclear interactions and from the peaks widening due to range straggling and energy spread [14]. The Delta R80 (i.e. difference between the proximal and distal depth positions where the dose is reduced to 80% of the peak maximum) is reported in Table 2. This value gives an indication of the beam energy spread. Additional information on the beam initial energy spread can be found in the work of Fracchiolla et al. [15], where results obtained using the proton beam in the treatment room of the Trento Proton Therapy Centre are presented. The comparison of Monte Carlo simulations with measured Bragg curves suggests that the energy spread as a percentage of the mean beam energy ranges between 0.7% (lowest energy) and 0.3% (highest energies). These values were obtained in a different room and minor differences might arise due to slightly different arrangements of the transport beam line connecting the to the separate branches. However, preliminary data obtained for the experimental beam line indicates a trend similar to the data collected in the gantries.

3.2. Beam spot profiles in air and envelope measurements

Beam spot shape and size in air were measured with the Lynx detector in the whole energy range between 70 and 228 MeV. The 2-dimensional intensity matrix returned by the Lynx software was then analysed, in order to extract profiles in the X–Y plane perpendicular to the beam direction. As shown in Fig. 3, the spots at the Isocenter are

Table 2
Parameters obtained from the Bragg curves plotted in Fig. 2. The distal and proximal R80 are reported, together with their differences as a function of the effective beam energy at Isocenter. The Peak-to-Plateau ratios are also show.

E (MeV)	Proximal R80 (cm)	Distal R80 (cm)	Delta R80 (cm)	Peak-Plateau ratio
68.5	3.87	3.72	0.15	4.67
98.6	7.52	7.20	0.32	4.40
117.8	10.31	9.88	0.43	4.33
141.7	14.29	13.74	0.55	4.20
158.0	17.28	16.64	0.64	4.18
178.2	21.30	20.5	0.80	3.94
201.1	26.22	25.32	0.90	3.85
222.9	31.30	30.25	1.05	3.55

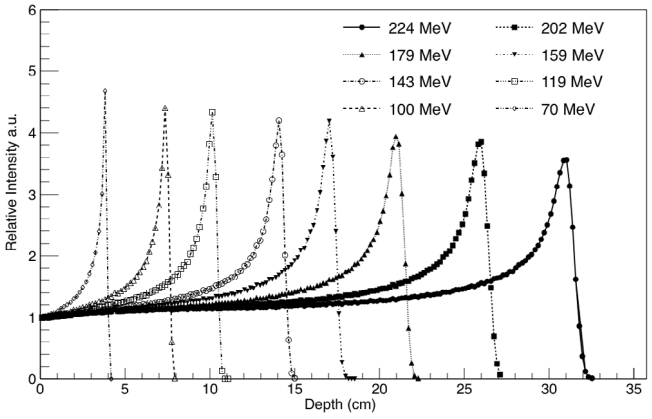

Fig. 2. Bragg curves measured at different energies with the Giraffe detector placed at the Isocenter position. Thanks to a previous calibration of the detector, the depth plotted on the X-axis is expressed as water-equivalent.

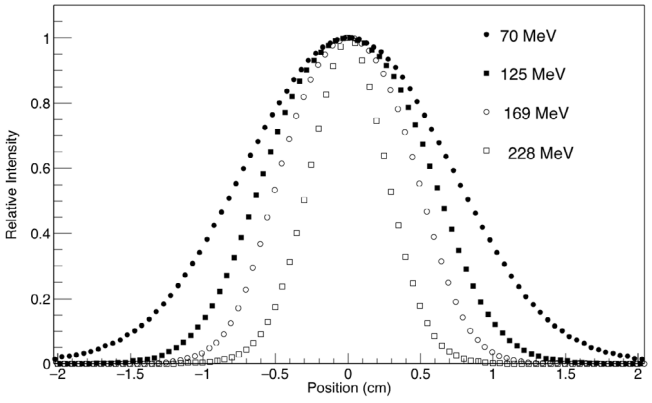

Fig. 3. Beam spot profiles measured at different energies with the Lynx detector placed at the Isocenter position.

characterized by a Gaussian profile defined by the following fit function:

$$f(x,\mu,\sigma) = \frac{1}{\sqrt{2\pi}\sigma} e^{-\frac{(x-\mu)^2}{2\sigma^2}} \quad (1)$$

where μ and σ refer to the centre and to the standard deviation of the Gaussian, respectively. The spot size as a function of the beam energy is summarized in Table 3. From the profile measured in both X and Y directions, the beam spatial asymmetry has been quantified according to the following formula:

$$\text{Spot Asymmetry}\,(\%) = \frac{\sigma_x - \left(\frac{\sigma_x+\sigma_y}{2}\right)}{\frac{\sigma_x+\sigma_y}{2}}. \quad (2)$$

Spot profiles have been also measured at different distances from the exit window, in order to investigate the so-called beam envelope (i.e. evolution of the beam transversal profile in air as a function of the distance from the exit window). The results for four representative energies are reported in Fig. 4 and show that the focal point is always obtained shortly after the exit window.

Table 3
Beam spot size estimated from a Gaussian fit on the profiles measured in the X–Y plane perpendicular to the beam direction. The spot asymmetry is calculated according to Eq. (1).

E (MeV)	σ_x (mm)	σ_y (mm)	Asymmetry (%)
70.2	6.93	6.91	0.1
73.9	6.63	6.74	0.8
82.7	6.28	6.41	1.0
90.8	6.04	6.15	0.9
100.0	5.63	5.73	0.8
105.6	5.42	5.63	1.8
112.4	5.26	5.43	1.6
119.0	5.05	5.24	1.9
125.3	4.90	5.09	1.9
131.3	4.70	4.88	1.9
137.2	4.49	4.79	3.2
142.9	4.50	4.62	1.3
148.5	4.39	4.52	1.4
153.9	4.23	4.41	2.0
159.2	4.10	4.31	2.5
164.4	4.02	4.19	2.0
169.4	3.93	4.08	1.8
174.4	3.85	4.07	2.7
179.3	3.76	3.92	2.1
184.1	3.71	3.84	1.7
188.8	3.66	3.83	2.2
193.4	3.57	3.74	2.2
197.9	3.48	3.64	2.3
202.4	3.44	3.52	1.1
206.9	3.33	3.44	1.5
211.2	3.33	3.31	0.4
215.5	3.18	3.19	0.1
219.8	3.10	3.08	0.5
224.0	3.04	2.97	1.0
228.2	2.74	2.72	0.2

3.3. Flux measurements

Due to the lack of on-line beam monitoring devices in the experimental room, the Mini-Q detector was employed to obtain information on the proton flux at different energies. For this purpose, the detector had to be calibrated to convert the counts provided by the integral chambers into number of protons. The calibration was performed in the medical treatment room, where it is possible to deliver a given number of monitor units (MU, i.e. a reference quantity correlated to the dose delivered by the machine and measured by ionization monitor chambers) corresponding to a given number of protons. For redundancy, a Faraday Cup was used as reference instrument for cross-calibration, collecting the integral charge and converting it into number of protons based on the electrometer read-out. By comparing the Mini-Q output with that of the Faraday Cup, it was possible to produce a look-up table of conversion factors (i.e. number of protons/integral chamber count) as a function of the proton beam energy. The results are summarized in Table 1, where the proton flux measured at the Isocenter as a function of the beam energy is reported. Those values correspond to the number of

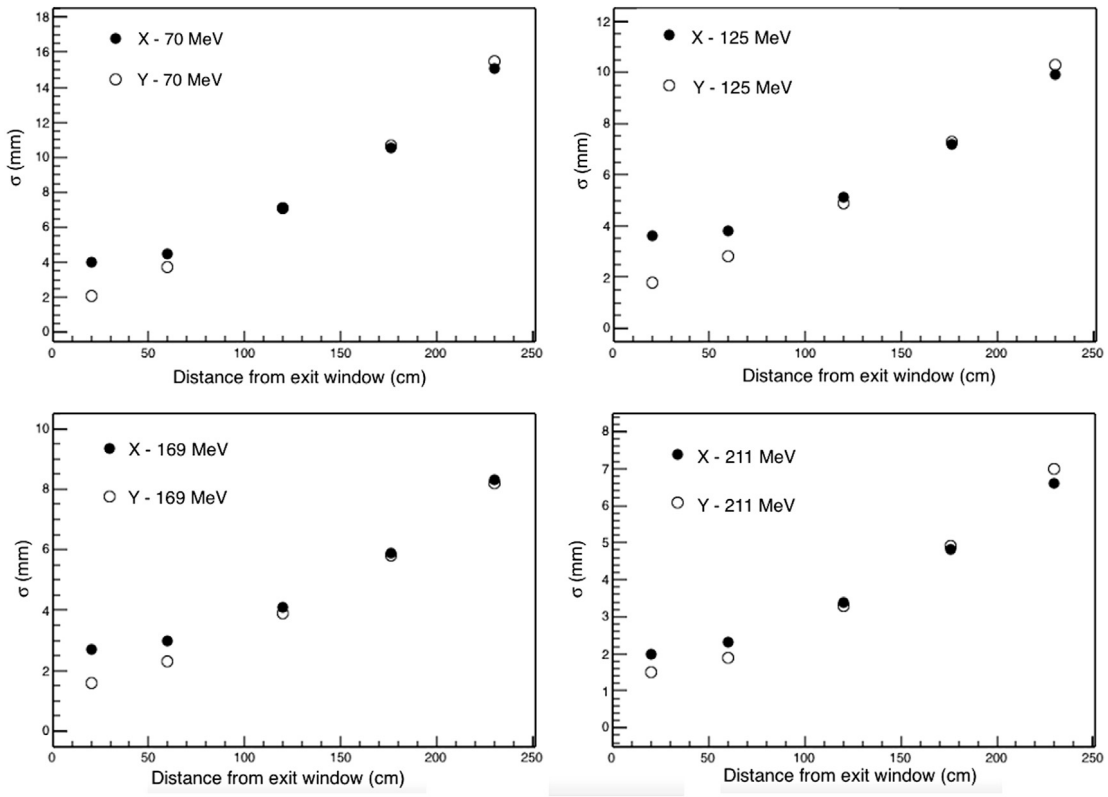

Fig. 4. Beam width in the X and Y profiled as a function of the distance from the beam exit window. The width is expressed as standard deviation of the Gaussian function used to fit the profiles.

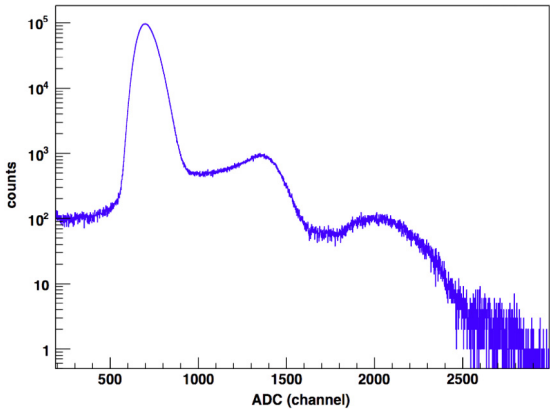

Fig. 5. Pulse-height spectrum of 148 MeV proton beam acquired with an ADC. The counts on the Y-axis are in logarithmic scale.

protons integrated over the beam profile for a requested beam current of 1 nA regardless of the energy. The range goes from about 3×10^6 particles/s at 70 MeV up to about 2×10^8 particles/s at the highest energy of 228 MeV. This trend reflects the energy-dependent transport efficiency of the beam line and indicates that a large portion of the beam is cut at the ESS for the lowest energy. These measurements provided an estimate of the transport efficiency ranging between about 0.1% and 10%, depending on the beam energy. According to the dynamic range provided by the cyclotron, these fluxes can be increased by a factor of 10^2 by increasing the accelerator output current up to about 320 nA.

The flux measurements at the low intensity regime have been performed with the basic data acquisition setup described above (see *Detectors* Section). The plastic scintillator was positioned at Isocenter, and the beam rate was recorded for different dark current settings (i.e. source high voltage and current parameters). The procedure was repeated at all available energies and the results proved that it was possible to gradually reduce the proton flux down to a rate of 10^1 particles per second. A fine-tuning of the beam rate is also possible but real-time feedback must be provided from the experimental room to the accelerator operators. Fig. 5 shows the pulse height spectrum for the 148 MeV beam. The main peak corresponds to single protons traversing the detector, while the two lower peaks on the right side are due to simultaneous hit of the detector by two or three primary particles (referred to also as double or triple hits, respectively). These events are recorded as a single event with energy deposition about twice or three times the value of a single proton. A quantitative analysis of the spectrum indicates that about 96% of the signal comes from single protons, while about 2% and 0.3% are associated to double and triple hits, respectively. We assume that the remaining fraction is produced by the background. The measurement was repeated at different proton beam energies and showed similar results.

4. Discussion and conclusions

A new experimental facility for high-energy proton beam irradiation is presented in this work. The characterization of the beam physical properties is the result of an extensive experimental campaign. The results include energy-on-target, spot size, beam envelope and flux measurements and represent an essential database for future experiments. The pencil beam provided at experimental room of the Trento Protontherapy centre has an energy range between 70 and 228 MeV and a spot size in-air between 6.9 and 2.7 mm sigma at the lowest and highest energies, respectively. Lower energies can be obtained by passive degraders added after the exit window. The flux dynamic range in air ranges between 10^1 and 10^{10} particles per second. This guarantees the possibility to perform a great variety of experiments from nuclear and particle physics, detector testing, test of shielding materials and radiation hardness.

The data obtained with the low intensity regime represent a proof-of-principle of the possibility to run a cyclotron built for medical purposes also at very low beam rates. Further studies are needed to investigate the beam initial energy spread. Imaging of the beam spot could not be accomplished at low intensities due to the limitations of the available detectors. However, we do not expect large deviations from what has been observed at the standard intensities because the beam optics is not affected by the technique adopted to reduce the intensity.

Several external groups had the opportunity to perform experiments in the facility during the first year of activities, as a part of both national and international collaborations, thus proving the interest of the scientific community for this facility [16,17]. Even if the centres dedicated to proton therapy are spreading worldwide, this trend is not translated into an increased availability of proton beams for research purposes. This can be explained by the obvious constraints related to the use of patient rooms for non-clinical purposes. In this context, experimental rooms fully dedicated to research activities represent an important opportunity for pre-clinical research as well as for studies aiming at technological developments. The scientific community has been expressing a growing interest for the construction and setup of research facilities placed side by side to clinical centres where it is possible to perform applied as well as basic research. This type of study can provide useful data and indications for this purpose.

While results concerning the Physics beam line are presented here, a different setup is needed for the Biology beam line. In this case, large fields (e.g. 10×10 cm^2) with high dose homogeneity (>90%) are necessary for performing radiobiological experiments. For this purpose, an ongoing effort for designing and realizing a passive scattering system, including extensive simulation studies, is being carried out at Trento proton therapy centre. Once available, the use of the second beam line will not be restricted to biological applications, but will be open to any activity requiring large field irradiations. A detailed description of the Biology beam line setup and characterization will be the topic of a separate publication.

The Trento irradiation facility complements a network of irradiation facilities available in the context of INFN, including the Intermediate Energy beam line (20–80 MeV/u) established at the LNS [5,6] and the high-energy ion beam experimental facility under construction at CNAO [7]. Once fully operational, this network will offer to the scientific community the possibility to perform experiments with all types of ion beams that are currently considered for therapeutic applications.

Acknowledgements

The authors are grateful to the Trento Provence and to the Healthcare Agency for their generous support to the construction of the experimental vault at the proton therapy centre. We would like to express our great appreciation to Prof. Renzo Leonardi for promoting the construction of the centre in Trento and for his foresight to include a vault dedicated to research with proton beams. We thank Carlo Civinini (INFN-Firenze, Italy) and his group for the support provided during the first low intensity tests. We also thank Giuseppe Battistoni (INFN-Milano) and the INFN-Roma 1 group for the fruitful discussions. We are grateful to the INFN groups of Torino (Italy) and Tor Vergata (Roma, Italy) and to the Biophysics Department of GSI (Darmstadt, Germany) for supplying equipment needed for the experiments.

Funding

This work was partially supported by the National Institute for Nuclear Physics (INFN) CSN5 Call “MoVe IT”.

References

[1] B. Rombi, et al., Implementation of Proton Therapy for pediatric tumors at the new proton facility in Trento, Pediatr. Blood Cancer 62 (2015) S352.
[2] A. Peters, et al. Operational status and further enhancements of the HIT accelerator facility, in: Proceedings of the International Particle Accelerator Conference, 2010, pp. 73–75.
[3] S. Helmbrecht, et al., Proton beams for physics experiments at Oncoray, Radiother. Oncol. 118 (2016) S60–S61.
[4] J. Swakon, et al., Proton radiotherapy facility for ocular tumors at the IFJ PAN Kraków Poland, Radiat. Meas. 45 (2010) 1469–1471.
[5] G. Russo, et al., Preliminary study for small animal preclinical hadrontherapy facility, Nucl. Instrum. Methods Phys. Res. A 846 (2017) 126–134.
[6] G.A.P. Cirrone, et al. A 62-MeV Proton Beam for the Treatment of Ocular Melanoma at Laboratori Nazionali del SUd-INFN 51 (2004) 860–865.
[7] M.G. Pullia, et al. The experimental beam line at CNAO, in: Proceedings of the International Particle Accelerator Conference, 2016, pp. 1334–1336.
[8] A. Smith, et al., The M.D. Anderson proton therapy system, Med. Phys. 36 (2009) 4068–4083.
[9] T. Kamada, et al., Carbon ion radiotherapy in Japan: an assessment of 20 years of clinical experience, Lancet Oncol. 16 (2015) e93–e100.
[10] S. Russo, et al., Dosimetric characterization of a commercial 2-D scintillation detector for quality assurance tests in scanned proton and carbon ion beams, Phys. Med. 32 (2017) 58–59.
[11] C. Bäumer, et al., Evaluation of detectors for acquisition of pristine depth-dose curves in pencil beam scanning, J. Appl. Clin. Med. Phys. 16 (2015) 151–163.
[12] S. Braccini, et al., Segmented ionization chambers for beam monitoring in hadron-therapy, Modern Phys. Lett. A 30 (2015) 1540026.
[13] E.W. Cascio, B. Gottschalk, A simplified vacuumless faraday cup for the experimental beamline at the Francis H. Burr proton therapy center, in: IEEE Radiation Effects Data Workshop, Piscataway, 2009, pp. 151–155.
[14] H. Paganetti, Proton Therapy Physics, CRC Press, 2011, pp. 53–54.
[15] F. Fracchiolla, et al., Characterization and validation of a Monte Carlo code for independent calculation in proton therapy treatments with pencil beam scanning, Phys. Med. Biol. 60 (2015) 8601–8619.
[16] G. Gallo, et al., QBeRT: an innovative instrument for qualification of particle beam in real-time, J. Instrum. 11 (2016) C11014.
[17] C. Civinini, et al. Proof-of-principle results of proton computed tomography, in: Proceedings of the IEEE Nuclear Science Symposium and Medical Imaging Conference, 2016, (in press).